Neurobiology of Disease 223 (2026) 107381

Contents lists available at ScienceDirect

Neurobiology of Disease

journal homepage: www.elsevier.com/locate/ynbdi

Longitudinal and combined assessment of 24(*S*)-hydroxycholesterol and Neurofilament light chain in the early stages of Huntington's disease

Lidia Sarro [a], Marta Valenza [b], Alessia Mongelli [a], Alice Passoni [c], Anna Castaldo [a], Monica Favagrossa [c], Laura Pasetto [c], Valentina Bonetto [c], Renzo Bagnati [c], Marina Grisoli [d], Anna Nigri [d], Giulia Birolini [b,e], Elena Zerbini [b], Simone Tomè [f,g], Marco Masseroli [f,g], Erika Salvi [g,h], Laura Colombo [c], Mario Salmona [c], Elena Cattaneo [b,e], Caterina Mariotti [a,*]

[a] *Fondazione IRCCS Istituto Neurologico Carlo Besta, via Celoria 11, 20133 Milan, Italy*
[b] *Department of Biosciences, University of Milan, via Celoria 26, 20133 Milan, Italy*
[c] *Istituto di Ricerche Farmacologiche Mario Negri IRCCS, via Mario Negri 2, 20156 Milan, Italy*
[d] *Unit of Neuroradiology, Fondazione IRCCS Istituto Neurologico Carlo Besta, via Celoria 11, 20133 Milan, Italy*
[e] *Istituto Nazionale di Genetica Molecolare "Romeo ed Enrica Invernizzi", via F. Sforza 35, 20122 Milan, Italy*
[f] *Politecnico di Milano, Department of Electronics, Informatics, and Bioengineering, via Ponzio 34/5, 20133 Milan, Italy*
[g] *Computational multi-Omics of Neurological Disorders (MIND) Lab, Fondazione IRCCS Istituto Neurologico Carlo Besta, via Celoria 11, 20133 Milan, Italy*
[h] *Data Science Center, Fondazione IRCCS Istituto Neurologico Carlo Besta, via Amadeo 42, 20133 Milan, Italy*

ARTICLE INFO

Keywords:
Oxysterol
NfL
Fluid biomarker
Cholesterol metabolites

ABSTRACT

Huntington's Disease (HD) is an autosomal dominant neurodegenerative disorder. Recent clinical research has focused on neurofilament light chain protein (NfL), and cholesterol metabolites as potential fluid biomarkers related to disease progression.

Our aim was to explore whether the combined longitudinal assessment of NfL and cholesterol-derived metabolites would improve the characterization of early HD stages.

We enrolled 96 HD individuals and 63 healthy controls. Disease stage of HD participants was determined using both the system based on Total Motor Score (TMS), and the new HD-Integrated Staging System (HD-ISS). Concentrations of plasma NfL, and cholesterol precursors and metabolites, were measured at baseline and 2-year follow-up.

In premanifest individuals, classified according to TMS, we found significantly reduced 24(*S*)-hydroxycholesterol (24S-OHC), a metabolite entirely derived from brain cholesterol catabolism, and normal level of NfL. When applying the HD-ISS, 24S-OHC was significantly reduced in HD-ISS-1 (25.6 ± 7.6 ng/ml) and HD-ISS-3 (30.5 ± 15.7) compared with controls (39.5 ± 14.1). NfL was increased in HD-ISS-1 (16.1 ± 6.5 pg/ml), HD-ISS-2 (16.1 ± 6.5) and HD-ISS-3 (27.0 ± 6.9) compared with controls (5.5 ± 1.7 pg/ml). In HD-ISS-0, all biomarker concentrations were similar to those of controls. At follow-up, NfL increased in HD-ISS-1 (+20%; $p < 0.005$). ROC analyses showed that NfL discriminated HD-ISS-0 and HD-ISS-1 from controls. 24S-OHC distinguished HD-ISS-1 from controls.

Plasma NfL and 24S-OHC concentrations provide complementary insights into early biological changes in HD, and holds the potential to characterize the transition phase from the pre-symptomatic to the early symptomatic stage.

1. Introduction

Huntington's Disease (HD) is an autosomal dominant neurodegenerative disorder caused by a pathological elongation of cytosine-adenine-guanine (CAG) tract (>35 CAG) in the *huntingtin* gene. The number of CAG repeats correlate with the age of onset, i.e. longer triplet expansions are associated with earlier clinical onset (Lee et al., 2019). For the majority of cases the symptoms of the disease become manifest in adulthood and are characterized by chorea/dystonia; cognitive decline and behavioral abnormalities (Dorsey, 2013). Disease course

* Corresponding Author: Caterina Mariotti, MD, Fondazione IRCCS Istituto Neurologico Carlo Besta.
E-mail address: caterina.mariotti@istituto-besta.it (C. Mariotti).

https://doi.org/10.1016/j.nbd.2026.107381
Received 4 February 2026; Received in revised form 31 March 2026; Accepted 2 April 2026
Available online 6 April 2026

was initially categorized into a pre-symptomatic phase (pre-HD), in which the gene mutation is present but motor symptoms have not yet manifested, and subsequent symptomatic phases in which disease severity progressively increases (Shoulson and Fahn, 1979; Marder et al., 2000). A refined characterization of the pre-symptomatic phase was attempted with mathematical models developed to estimate the age of onset based on CAG repeat length. These models transformed the concept of a unique pre-symptomatic phase, and allowed the stratification of HD mutation carriers according to their proximity to motor onset (i.e. far/close to onset) (Langbehn et al., 2004; Langbehn et al., 2010). The estimated prediction of time-to-onset allowed longitudinal studies on premanifest individuals and the identification of early clinical and biological changes even in the absence of overt motor symptoms (prodromal phase).

Based on these acquisitions, a novel Huntington's Disease Integrated Staging System (HD-ISS) has been recently proposed, in which the full course of HD is divided in four consecutive stages taking into consideration actual genetic, neuroimaging, cognitive, and clinical characteristics (Tabrizi et al., 2022). Individuals categorized in HD-ISS stage 0 carry the *HTT* gene mutation in the absence of clinical symptoms or detectable MRI abnormalities, while evidence of basal ganglia atrophy at MRI defines the HD-ISS stage 1. HD-ISS stage 2 individuals show initial phenotypic changes captured by scores on the Unified Huntington's Disease Rating Scale-Total Motor Score (HDRS-TMS) and on Symbol Digit Modality Test (SDMT), while individuals in HD-ISS stage 3 show clinical motor signs, reduction of functional capabilities (TFC score), and of independence score (IS) (Tabrizi et al., 2022).

A further step in clinical research consisted in the identification of fluid biomarkers that could complement clinical measures in monitoring disease progression and response to therapies. Several biomarkers have been explored in recent cohort studies, and the 24(*S*)-hydroxycholesterol (24S-OHC) and neurofilament light protein (NfL) appear to be among the most promising candidates. NfL is the smallest of the three subunits of the neurofilaments constituting the neuronal cytoskeleton (Rosengren et al., 1996). Elevated NfL levels have been shown to correlate with disease severity and progression in several neurological and neurodegenerative conditions; including Alzheimer's disease; amyotrophic lateral sclerosis; and multiple sclerosis (A Virata et al., 2024). NfL levels were also found to be increased in plasma and cerebrospinal fluid (CSF) of HD symptomatic patients and pre-HD individuals (Byrne et al., 2017; Byrne et al., 2018; Johnson et al., 2018; Rodrigues et al., 2020; Scahill et al., 2025; Rodrigues et al., 2021; Parkin et al., 2021; Parkin et al., 2023; Parkin et al., 2024).

The 24S-OHC is a catabolite of cholesterol exclusively derived from cerebral tissue. In fact, given that cholesterol does not cross the blood-brain barrier (BBB), plasma cholesterol levels reflect dietary intake and hepatic synthesis, but not brain cholesterol metabolism. In humans brain cholesterol is nearly completely synthesized de novo in the brain by the astrocytes, and is eliminated through its conversion to the hydrophilic catabolite 24S-OHC, which can cross the BBB and can be detected in peripheral blood. Consequently, this molecule can serve as a specific marker of brain cholesterol homeostasis in humans (Björkhem et al., 1998).

In HD, we firstly demonstrated that both symptomatic and premanifest individuals have decreased plasma 24S-OHC levels in comparison with controls (Leoni et al., 2008; Leoni et al., 2011; Leoni et al., 2013). Consistently, reduced brain and plasma levels of 24S-OHC have also been reported in several HD mouse models, further supporting its value as a translational biomarker of altered cholesterol metabolism (Valenza et al., 2023). Reduced concentrations of 24S-OHC have been also described in Alzheimer's disease (Gamba et al., 2021); Parkinson's disease (Huang et al., 2019); spinocerebellar ataxias (Locci et al., 2022); and recently confirmed in large cohorts of HD patients participating in on HD multicentre natural history studies (Gray et al., 2024).

Although there is an extensive literature regarding NfL24 and 24S-OHC plasma concentration in various neurological diseases, this is the first study, to our knowledge, evaluating in the same patient population the plasma levels of NfL, total cholesterol, and its peripheral and brain-derived catabolites. Moreover, the disease stage of our participants was determined using both the original HD staging system and the new HD-ISS, allowing a better characterization of the earliest HD stages. Our aim was to correlate 24S-OHC and NfL levels with the progression of clinical measures and to explore whether their combined assessment and longitudinal changes could improve the monitoring of early disease stages.

2. Methods

2.1. Participants

Study participants were consecutively enrolled among patients and family members attending the HD-clinical center of our Institute. Inclusion criteria were: age $\geq$ 18 years; repeat expansion in *HTT* gene $\geq$38 triplets; Total Functional Capacity (TFC) score $>$ 4 points; capability of providing written informed consent. Subjects presenting severe cognitive or behavioral disturbances, or major concomitant diseases other than HD were excluded. HD participants and age-matched healthy controls underwent neurological examination, volumetric brain MRI, and blood withdrawal for determination of oxysterols, cholesterol precursors, and NfL plasma levels. Clinical evaluation included the Unified Huntington Disease Rating Scale with Total Motor Score (UHDRS-TMS), as well as Cognitive and Functional scores (https://www.euro-hd.net/html/network). Symptomatic HD patients and pre-HD mutation carriers were classified in disease-stages according to two different systems: (a) the method based on UHDRS-TMS score and Total Functional Capacity score (TMS/TFC staging system) (Shoulson and Fahn, 1979; Marder et al., 2000), and (b) the novel HD-ISS (Tabrizi et al., 2022). In the TMS/TFC staging system, the groups are named pre-HD, HD-I, HD-II and HD-III. In the HD-ISS, the groups are named HD-ISS 0; 1; 2; 3.

The estimated years to disease motor onset were calculated according to the method described by Langbehn et al. (mean age[CAG] = 21.54 + Exp(9.556–0.1460CAG) (Langbehn et al., 2004). The CAP score (CAG-Age-Product) was also used as a predictor of proximity to clinical onset (Warner et al., 2022). Clinical evaluation, blood sampling, and neuroimaging were repeated at 2-year follow up. The study was approved by the local ethics committee (Protocol N. 50; 11 Aprile 2018) and written informed consent was obtained from all participants in accordance with the Declaration of Helsinki.

2.2. Biochemical analyses

Blood samples (6 ml) were collected after overnight fasting. We measured the plasma levels of (1) total cholesterol, reflecting extracerebral synthesis, (2) cholesterol precursors 7-dehydroxy-cholesterol (7DHC) and desmosterol, (3) the 27-hydroxycholesterol (27OHC), produced in peripheral tissues through a hydroxylation reaction of cholesterol by the enzyme CYP27A1, and (4) the 24-hydroxycholesterol (24S-OHC), produced in the brain by the conversion of cholesterol to the hydrophilic catabolite 24S-OHC by the neuronal-specific enzyme CYP46A1.

Plasma determination of cholesterol and its metabolites was performed according to the method described in details Passoni et al (Passoni et al., 2024). NfL plasma levels were measured with the single-molecule array (Simoa NF-light™ Advantage – SR-X) and SR-X Analyzer, according to manufacturer instructions.

2.3. Brain MRI

Structural MRI data were acquired using an Achieva dStream 3 T-MR scanner (Philips Healthcare BV, Best, NL) equipped with a 32-channels head coil. A 3D T1-weighted (T1w) structural sequence (TR = 8.17 ms, TE = 3.7 ms, FOV = 240 × 240 mm^2, voxel size = 1x1x1 mm^3, flip angle = 8°,180 sagittal slices) and a 3D T2-FLAIR sequence (TR = 4800

ms, TE = 293 ms, TI = 1650 ms, FOV = 240 × 240 mm^2, voxel size = 1x1x1 mm^3, 180 axial slice) were acquired.

First, cortical segmentations were conducted with FreeSurfer software (v. 6), using both T1w and T2-FLAIR images. Visual inspection and manual correction were conducted by an expert operator on the output. Each subject was resampled into a surface standard space derived from Montreal Neurological Institute (MNI 305) (Fischl et al., 1999) and spatial smoothing was applied. The mean of the left and right measures of subcortical nuclei was computed, and all volumes were expressed as percentage of total intracranial volume. Brain MRI was not performed in case of claustrophobia or severe choreic movements.

2.4. Statistical analysis

For statistical analyses of plasma measurement of oxysterols and cholesterol precursors, the Multivariate Robust principal component analysis was applied for removal of outliers. The 24-OHC levels from three HD individuals were excluded from statistical analyses, as they were considered outliers based on Multidimensional test (Mahalanobis distance). Group differences in clinical and biochemical variables among cohorts of subjects at different disease stages (using both staging categorizations) were assessed using the Kruskall-Wallis nonparametric test, followed by the post-hoc non-parametric Dunn test for all pairs multiple comparisons. Receiver Operating Characteristic (ROC) Curve were performed to assess the discriminative ability of 24S-OHC and NfL in distinguishing between controls and early HD-ISS stages, and optimal cut-off values were determined by the Youden Index. Correlations were assessed using the nonparametric Spearman test. Longitudinal trajectories for 24S-OHC and NfL were assessed using Wicoxon paired-test. All analyses were carried out using GraphPad Prism (version 10), JMP (version 17), and R (version 4.3.2). A significance threshold of $p < 0.05$ was applied.

3. Results

3.1. Recruitment of participants and clinical classification

From October 2019 to March 2023, we recruited 159 study participants: 96 HD individuals, and 63 age-matched healthy controls. According to the TMS/TFC-based staging system, HD participants were classified as follows: pre-HD ($N = 39$; TFC 13; TMS ≤5); HD-I ($N = 32$; TFC 11–13; TMS ≤5); HD-II ($N = 13$; TFC 7–10); and HD-III ($N = 12$; TFC 6–3).

According to the novel HD-ISS, the HD participants were reassigned as: HD-ISS-0 ($N = 21$); HD-ISS-1 (N = 13); HD-ISS-2 (N = 13); and HD-ISS-3 ($N = 49$) (Fig. 1).

The most significant effect of the reclassification was observed in the pre-HD group. In fact, 21 of 39 (54%) pre-HD individuals were assigned to HD-ISS-0, 13 (33%) were assigned to HD-ISS-1, and 5 individuals (13%) to HD-ISS-2. Most individuals in HD-I (75%) and all patients in HD-II and HD-III were reassigned to HD-ISS-3 (Fig. 1).

3.2. Biochemical analyses

We first analyzed clinical and biochemical data using the stratification of HD participants based on TMS staging system (**Supplementary Table 1**). The levels of circulating total cholesterol, 7-dehydrocholesterol, desmosterol, and 27-hydrocholesterol (27OHC) were similar between controls and all HD cohorts. In contrast, plasma levels of 24S-OHC, reflecting brain cholesterol metabolism, differed significantly

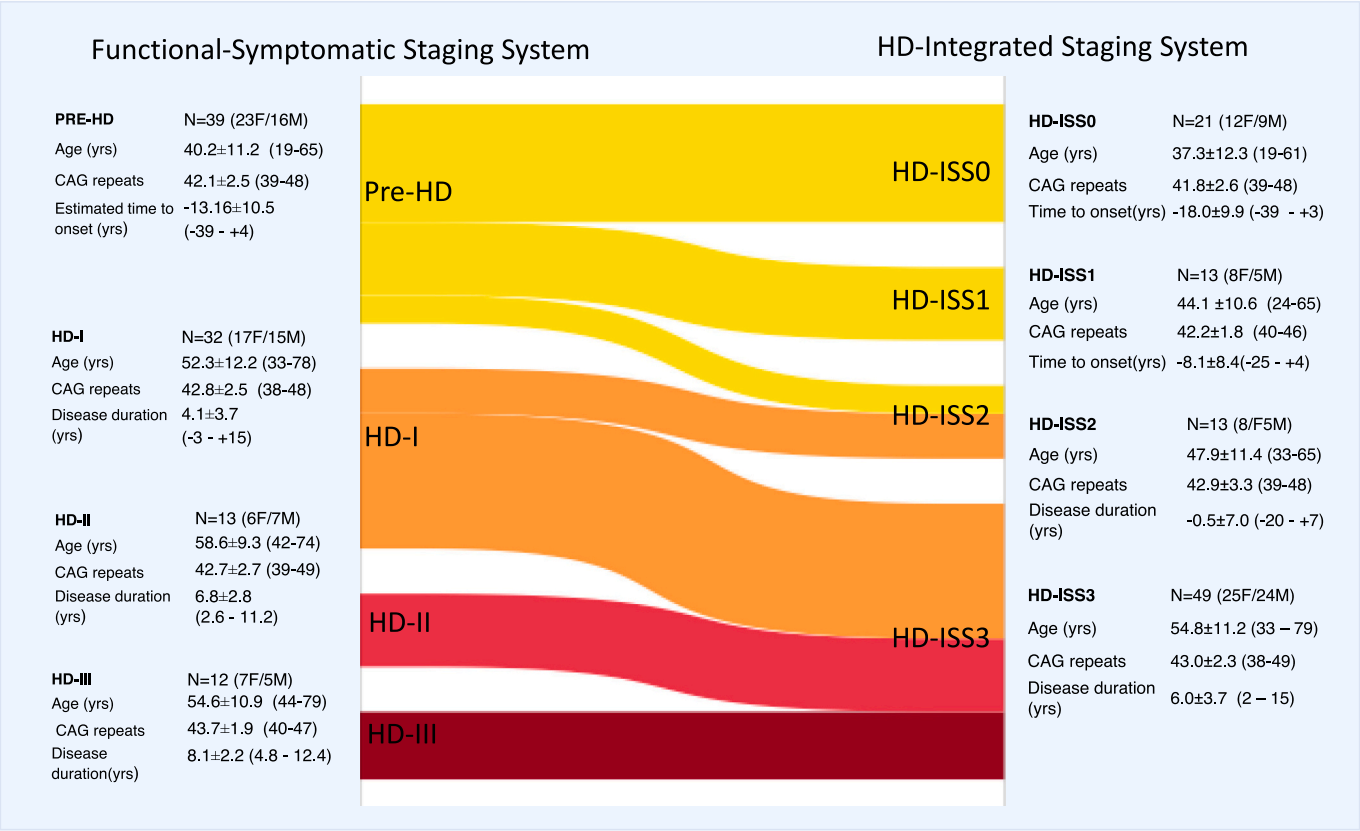

Fig. 1. Flow-chart showing motor-functional classification versus HD-ISS classification Schematic representation of the individuals participating in the study. In the left panel participants are categorized in different disease stages according to motor score (TMS) and total functional capacity score (TFC). In the right panel, the same population has been categorized according to the recent Huntingtons Disease Integrated Staging System (HD-ISS). All data are reported as mean ± SD (range). Healthy Controls were $N = 63$ individuals; F/M = 37/26; mean age 41.4 ± 14.5 (22–76) years.

among controls and HD groups ($p = 0.001$, Kruskal-Wallis test). The 24S-OHC concentration was 39.5 ± 14.1 ng/ml in controls, and were reduced in pre-HD individuals (31.4 ± 14.6 ng/ml; $p = 0.03$), in HD-I (34.4 ± 22.1 ng/ml; p = n.s.), and in HD-III (25.3 ± 7.5 ng/ml; $p = 0.008$) (Fig. 2A). The findings of lower 24S-OHC in symptomatic HD stages are consistent with those reported in all our previous cross-sectional studies in independent cohorts of patients (Leoni et al., 2008; Leoni et al., 2011; Leoni et al., 2013). In pre-HD, however, we previously observed lower 24S-OHC in near-to-onset and mid-form onset individuals (Leoni et al., 2013); but we found no difference with controls when pre-HD individuals were analyzed as a unique group including individuals close and far to motor onset (Leoni et al., 2008; Leoni et al., 2011). **(Supplementary Fig. 1)**.

When we used the HD-ISS classification, allowing a more precise definition of pre-HD cohorts, we observed that 24S-OHC level was significantly reduced in HD-ISS-1 ($p < 0.02$) and HD-ISS-3 ($p < 0.002$) in comparison with controls. In the HD-ISS-0, representing the earliest and fully premanifest stage, the 24S-OHC did not differ from controls (Table 1**;** Fig. 2B). This finding supports the hypothesis that in pre-manifest individuals the variability in 24S-OHC largely mostly reflects differences in group categorization.

The levels of NfL, a peripheral marker of axonal damage, were significantly increased in all symptomatic HD groups, categorized using the TMS staging system. NfL was 5.5 ± 1.7 pg/ml in controls, it increased to 26.1 ± 7.2 pg/ml in HD-I, 26.1 ± 5.5 pg/ml in HD-II; and 28.2 ± 7.9 in HD-III pg/ml ($p < 0.0001$for all in comparison with controls). Our results mirror those reported in other cohorts, showing 5–6 fold higher NfL concentrations in HD versus controls (Byrne et al., 2017; Parkin et al., 2024). However, we found no significant differences between symptomatic stages HD-I, HD-II, and HD-III. In the pre-HD population the mean NfL concentration was 11.8 ± 6.7 pg/ml, and it did not reach statistical significant difference from controls. (Fig. 2C**).**

When applying the HD-ISS classification, NfL levels were significantly increased in HD-ISS-1 ($p = 0.03$), HD-ISS-2 ($p = 0.0004$), and HD-ISS-3 ($p < 0.0001$) compared with controls, whereas no difference was observed between controls and HD-ISS-0 (Fig. 2D). Moreover, NfL concentrations showed a gradual increase across symptomatic stages, with a significant difference between HD-ISS-1 and HD-ISS-3 ($p < 0.04$) (Fig. 2D). This progressive pattern was not apparent using the TMS/TFC-based system, and it was highlighted with the HD-ISS framework that captures disease progression with greater sensitivity.

To assess the sensitivity and specificity of 24S-OHC and NfL in distinguishing between controls and early HD-ISS stages, ROC analyses were performed. Baseline 24S-OHC concentrations did not discriminate between controls and HD-ISS-0 (AUC = 0.5718; $p = 0.3264$; Fig. 3A) nor between HD-ISS stage 0 and stage I (AUC = 0.6703; $\boldsymbol{p = 0.0993}$; Fig. 3C**).** However, 24S-OHC concentrations effectively distinguished controls from HD-ISS stage 1 (AUC = 0.8083, $p = 0.0005$) **(**Fig. 3B**),** with an optimal cut-off value of 32.18 ng/ml (Youden Index).

In contrast, NfL concentrations showed a stronger discriminative ability. ROC analyses revealed that NfL could significantly distinguish controls from HD-ISS 0 (AUC = 0.7063; $p = 0.0256$) with an optimal cut-off value of 7.5 pg/ml (Fig. 3D), and controls from HD-ISS 1 (AUC = 0.9542, $p < 0.0001$) with an optimal cut-off value of 7.4 pg/ml

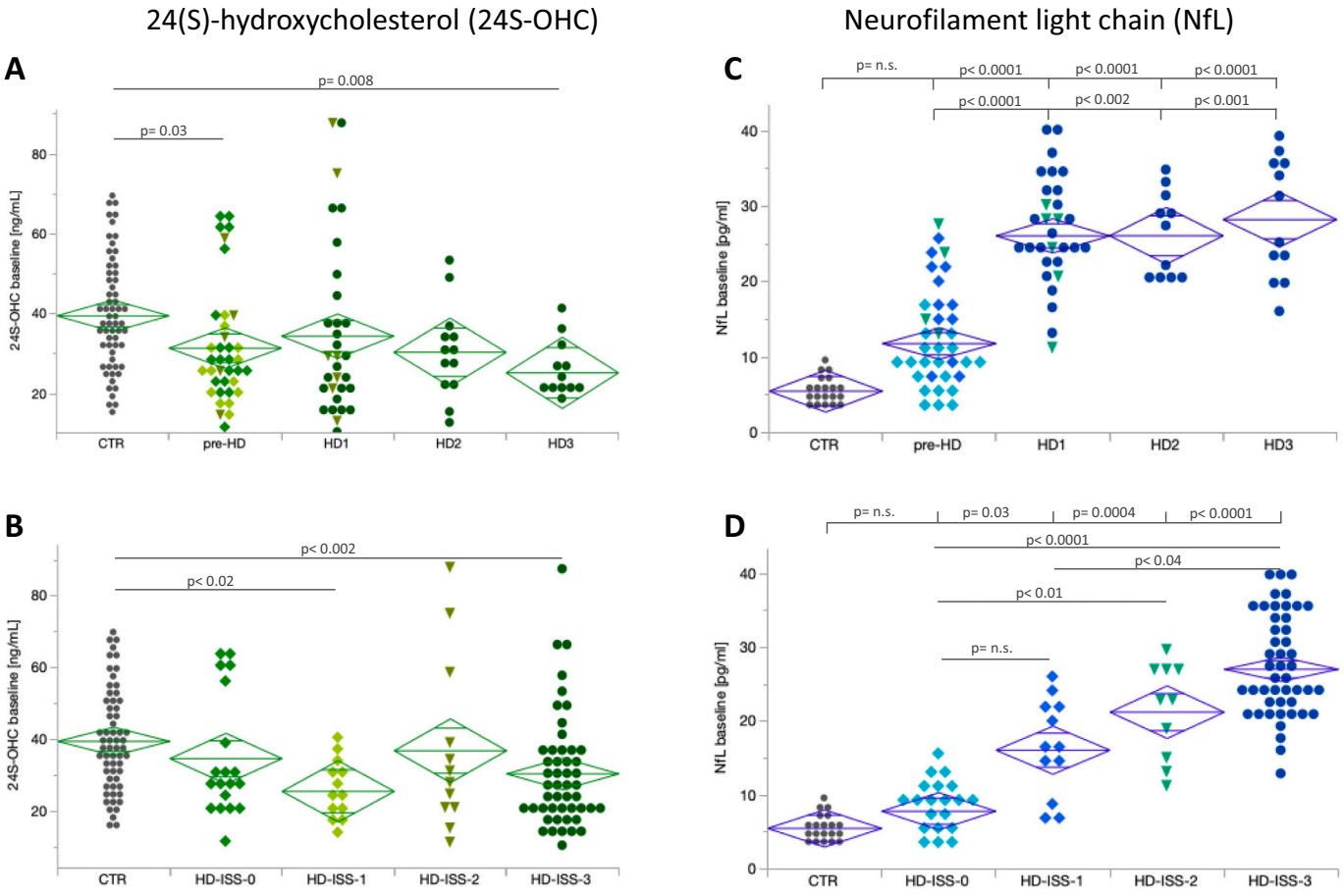

Fig. 2. Baseline 24S-OHC and NfL plasma levels in HD groups and in controls 24S-OHC plasma levels in HD individuals classified on the basis of total motor score and functional capacity score (**graph a**) and on the basis of the Huntingtons Disease Integrated Staging System (**graph c**). Graphs **b** and **d** show the NfL plasma levels in the same HD groups. Diamon lines represent the mean and CI 95%. Significant differences have been identified by Kruskall-Wallis non parametric test, followed by the post-hoc non-parametric Dunn test for all pairs multiple comparisons.

Table 1
Biochemical and clinical data in controls patients groups (according to the HD-Integrated Staging System-ISS).

	Healthy Controls	HD-ISS stage 0	HD-ISS stage 1	HD-ISS stage 2	HD-ISS stage 3
	N = 63	N = 21	N = 13	N = 13	N = 49
Clinical/ Cognitive scores	Mean ± SD -[Median]	Mean ± SD -[Median]	Mean ± SD -[Median]	Mean ± SD -[Median]	Mean ± SD -[Median]
UHDRS-TMS	0.2 ± 0.4 [0]	0.5 ± 0.9 [0]	1.5 ± 1.3 [2]	10.7 ± 11.6* [5]	33.3 ± 14.8*** [29]
UHDRS-TFC	13	13	13	13	9 ± 2.9*** [10]
MMSE	29 ± 1.1 [29]	28.9 ± 1.2 [29]	29.3 ± 1.1 [30]	28.8 ± 1.1 [29]	25.0 ± 3.5*** [25.5]
SDMT	48.2 ± 10.3 [47]	51.0 ± 10.2 [50]	51.7 ± 14.2 [51]	36.4 ± 11.5 [35]	18.8 ± 11.3*** [16]
Stroop Word Reading test	105.6 ± 14.8 [103]	104.7 ± 15.3 [105]	101.9 ± 18.9 [100]	82.8 ± 15.3 [84.5]	54.2 ± 24.1*** [50.5]
MRI					
Caudate volume *% TIV*	0.5 ± 0.05 [0.5]	0.5 ± 0.06 [0.5]	0.4 ± 0.04 [0.4]	0.4 ± 0.05* [0.3]	0.3 ± 0.06*** [0.3]
Putamen volume *% TIV*	0.7 ± 0.07 [0.7]	0.7 ± 0.1 [0.6]	0.5 ± 0.06* [0.5]	0.5 ± 0.08** [0.5]	0.4 ± 0.1*** [0.4]
Cholesterol and metabolites					
Total cholesterol *mg/ml*	1.7 ± 0.3 [1.6]	1.5 ± 0.3 [1.5]	1.4 ± 0.3 [1.4]	1.5 ± 0.3 [1.6]	1.6 ± 0.3 [1.7]
7-Dehydrocholesterol *ng/ml (cholesterol precursor)*	310.0 ± 250.9 [232.5]	175.4 ± 202.0 [146.5]	198.7 ± 131.1 [210.9]	363.7 ± 372.4 [283.8]	711.2 ± 833.0 [252.8]
Desmosterol ng/ml *(cholesterol precursor))*	298.9 ± 129.4 [257.9]	302.8 ± 169.9 [278.4]	285.0 ± 113.3 [302.1]	279.9 ± 179.8 [263.9]	345.0 ± 322.2 [259.8]
27-Hydroxycholesterol ng/ml *(peripheral cholesterol catabolite)*	111.9 ± 61.1 [106.3]	67.2 ± 43.9 [49.9]	65.2 ± 38.4 [65.8]	73.4 ± 48.6 [41.2]	98.2 ± 48.5 [95.5]
24-Hydroxycholesterol ng/ml *(brain derived cholesterol catabolite)*	39.5 ± 14.1 [37.7]	34.7 ± 17.0 [28.2]	**25.6 ± 7.6*** [25.4]	36.9 ± 24.3 [28.1]	**30.5 ± 15.7**** [26.1]
Neurofilament Light Chain					
NfL *pg/ml (N = 20)*	5.5 ± 1.7 [5.2]	7.8 ± 3.4 [7.7]	**16.1 ± 6.5*** [15.3]	**21.2 ± 6.9**** [22.9]	**27.0 ± 6.9***** [25.3]

UHDRS: Unified Huntington Disease Rating Scale; TMS: Total motor score; MMSE: Mini-Mental State Examination; TFC: Total Functional Capacities; SDMT: Symbol Digit Modalities Test; TIV: Total Intracranial Volume. Group differences were assessed by Kruskal–Wallis test followed by Dunn's post-hoc test. Asterisks denote significant pairwise differences with controls. *** $p < 0.0001$; **$p < 0.002$; *$p < 0.05$.

(Figs. 3E**)**. Furthermore, NfL concentrations effectively differentiated HD-ISS 0 from HD-ISS 1 (AUC = 0.8375; $p = 0.0016$) with an optimal cut-off value of 14.15 pg/m-l (Fig. 3F**)**.

3.3. Association between biochemical and clinical measures

We confirmed significant positive associations between NfL plasma levels and TMS, and with CAP scores, and negative associations with SDMT, the Stroop Word Reading test, and caudate and putamen volumes (Byrne et al., 2017; Parkin et al., 2021; Parkin et al., 2023) (**Supplementary Fig. 2**). These correlations remained statistically significant even after excluding premanifest subjects in HD-ISS 0 from the analysis. Conversely, the present study did not replicate the correlations between plasma 24S-OHC and clinical or imaging measures, described in previous reports by Leoni (Leoni et al., 2008; Leoni et al., 2011; Leoni et al., 2013). This discrepancy likely reflects several technical and analytical factors, including sample size, patient group composition, differences in biochemical assay methodologies, higher image quality images at 3 T MRI, and the non-linear biological changes of 24S-OHC during disease progression.

3.4. Longitudinal changes at 2-year-follow up

Baseline and 2-year follow-up evaluations were available for 19 controls and 81 HD individuals.

Individuals in HD-ISS-0 ($N = 19$) showed no longitudinal changes in clinical or volumetric brain MRI measures. In HD-ISS-1 ($N = 13$), we observed a significant increase in TMS and a decrease in putamen volume. Patients in HD-ISS-2 ($N = 12$) showed a significant decrease in SDMT score and caudate volume, while patients in HD-ISS 3 ($N = 37$) demonstrated significant worsening in TFC and the Stroop Word Reading test. Notably, plasma concentrations of total cholesterol and its precursor 7DHC showed significant longitudinal increase in HD-ISS-3. This observation may reflect a possible aging effect and increased synthesis in peripheral tissues (Table 2).

At 2-year follow-up, five individuals exhibited clinical or neuroimaging changes that led to a reassignment to a different HD-ISS stage. One individual shifted from HD-ISS-0 to HD-ISS-1 due to decreased putamen volume; two individuals transitioned from HD-ISS-1 to HD-ISS-2 because of TMS score > 5; and two individuals from HD-ISS-2 to HD-ISS-3 due to a decrease in TFC and an in independence score.

The concentrations of 24S-OHC showed no significant longitudinal changes in any of the HD-ISS groups (Table 2). In contrast, NfL concentrations significantly increased in individuals belonging to the HD-ISS-1, but not in patients in the other HD-ISS stages (**Supplementary Fig. 3**).

4. Discussion

We investigated the 2-year temporal dynamics of plasma 24S-OHC and NfL in a large cohort of HD individuals, aiming to evaluate and compare the combined contribution of these biomarkers in monitoring critical stages of disease progression. To our knowledge, this is the first longitudinal study combining the evaluation of these two plasma biomarkers in a study population classified according to both TMS/TFC-based staging system (Shoulson and Fahn, 1979; Marder et al., 2000) and the novel HD-ISS[7].

Both NfL and 24S-OHC are well-known candidate biomarkers that have been extensively investigated across several neurodegenerative diseases.

Plasma NfL levels closely reflect the extent of neuroaxonal damage and have been used to monitor disease progression. Recently, FDA and EMA have endorsed plasma NfL as a qualified outcome measure in clinical trials for amyotrophic lateral sclerosis and pediatric

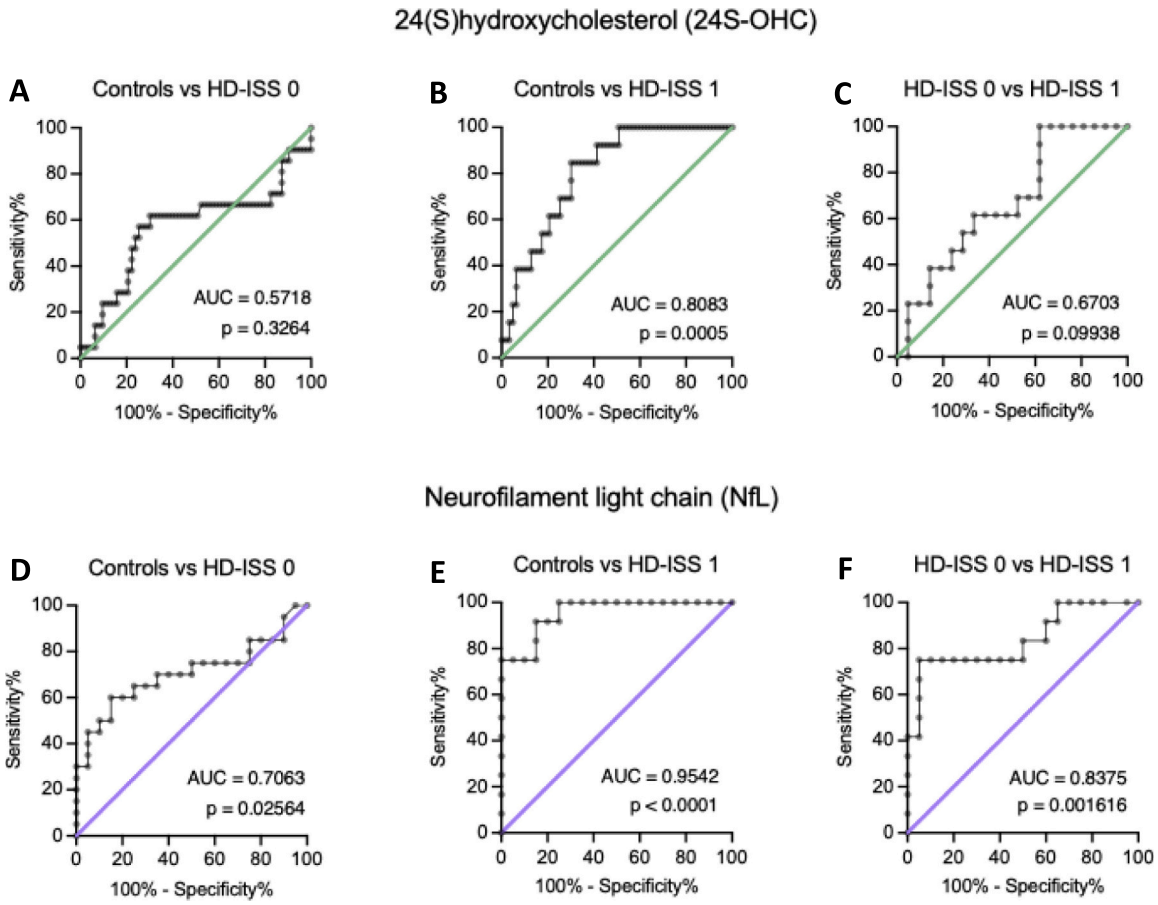

Fig. 3. Receiver operating characteristic (ROC) curve analyses for 24S-OHC and NfL ROC curve for baseline 24S-OHC analyzing effective discrimination between: (**a**) controls and HD-ISS stage 0; (**b**) controls and HD-ISS stage 1; (**c**). HD-ISS stage 0 and HD-ISS stage 1. The same type of analyses has been conducted for NfL plasma levels (**d, e, f**).

neurological diseases (Khalil et al., 2018; Miller et al., 2022).

Plasma 24S-OHC originates predominantly from the catabolism of brain cholesterol (Björkhem et al., 1998; Tripodi et al., 2024). In the adult brain, cholesterol is mainly synthesized by astrocytes and subsequently taken up by neurons through the LRP1 receptor. Within neurons, excess cholesterol is converted by the neuronal-specific enzyme cholesterol 24-hydroxylase (CYP46A1) into 24S-OHC, which readily crosses the BBB and is subsequently cleared into the circulation (Valenza et al., 2023). We found that plasma concentrations of 24S-OHC were significantly reduced in symptomatic HD patients in comparison with controls (Leoni et al., 2008; Leoni et al., 2011; Leoni et al., 2013; Gray et al., 2024), whereas total cholesterol, cholesterol precursors (7DHC, and desmosterol), and 27OHC, produced by peripheral cholesterol catabolism, were similar in controls and in HD population.

In HD symptomatic patients, we also confirmed a significant increase of NfL concentrations in comparison with controls (Byrne et al., 2017; Byrne et al., 2018; Rodrigues et al., 2020; Scahill et al., 2025; Rodrigues et al., 2021; Parkin et al., 2021; Scahill et al., 2020; Parkin et al., 2022; Li et al., 2023).

In premanifest HD individuals, 24S-OHC was found to be significantly reduced in some study population (Leoni et al., 2013); whereas in others cohorts the values were similar to those in controls (Leoni et al., 2008; Leoni et al., 2011; Gray et al., 2024).

Similarly, increased NfL levels have been detected in some pre-HD cohorts (Byrne et al., 2017; Scahill et al., 2020; Li et al., 2023), whereas in other pre-HD populations the concentrations were found to be comparable to age-matched controls (Parkin et al., 2021; Parkin et al., 2023; Voysey et al., 2024).

In the present study we found that pre-HD individuals, categorized according with the TMS/TFC staging system, had decrease 24S-OHC, and normal concentrations of NfL.

A possible explanation for these discrepancies lies in the earliest categorization system of pre-HD individuals that takes into account only the absence of overt motor symptoms. In contrast, the recently introduced HD-ISS provides a more granular classification of the presymptomatic individuals. In fact, asymptomatic individuals with normal neuroimaging findings are categorized as HD-ISS-0, while asymptomatic individuals with basal ganglia atrophy are categorized as HD-ISS-1. In our study, HD-ISS-0 individuals had plasma NfL levels similar to those of controls, whereas individuals in HD-ISS-1 group had significantly increase NfL levels. Consistent with our results, Parkin et al (Parkin et al., 2023). also reported increased NfL levels in HD-ISS-1 and proposed its potential use as a prognostic biomarker to refine stage classification within this early disease phase.

Considering the HD-ISS classification, the 24S-OHC displayed a pattern opposite to that of NfL. In fact, 24S-OHC concentrations were comparable to those of controls in HD-ISS-0, and were significantly reduced HD-ISS-1. These findings support the association of biomarkers changes with early volumetric brain changes detectable by MRI.

The temporal dynamics of NfL and 24S-OHC across disease stages showed that only NfL increased at 2-year follow-up, exclusively in the HD-ISS-1 group. No longitudinal changes were observed in the other HD-ISS stages. (Table 2).

Previous longitudinal studies reported progressive increases in NfL over time in both pre-symptomatic and manifest HD (Byrne et al., 2017; Li et al., 2023; Voysey et al., 2024). However, in those studies, HD-ISS-0 and HD-ISS-1 individuals were analyzed as a single group, and individual trajectories across early stages were not characterized (Parkin

Table 2
Clinical and biochemical measures at 2-year longitudinal follow-up in patient groups (according to HD-Integrated Staging System-ISS).

	HD-ISS stage 0		**HD-ISS stage1**		**HD-ISS stage 2**		**HD-ISS stage 3**	
	N = 19	Difference between BL-FU	N = 13	Difference between BL-FU (	N = 12	Difference between BL-FU	N = 37	Difference between BL-FU (
Clinical/ Cognitive scores	Mean ± SD	(%)	Mean ± SD	%)	Mean ± SD	(%)	Mean ± SD	
UHDRS-TMS score	0.7 ± 1.2	+30%	4.4 ± 5.4	**+185.0%***	16.8 ± 14.3	**+57.0%*****	44.5 ± 20.9	+%)**34.3%*****
UHDRS-TFC score	13 ± 0	0	13 ± 00	0	12.8 ± 0.4	−1.3%	7.1 ± 3.1	**−17.2%*****
MMSE score	29.0 ± 1.4	+0.2%	29.2 ± 1.3	−0.5%	28.4 ± 1.4	−1.0%	23.9 ± 5.5	−4.0%
SDMT score	51.2 ± 8.6	+2.4%	52.6 ± 16.0	+1.8%	34.0 ± 9.7	**−9.9%****	17.5 ± 16.5	−9.0%
Stroop Word Reading test score	100.1 ± 17.4	−1.3%	103 ± 14.7	+1.1%	76.9 ± 17.3	−8.4%	44.8 ± 26.2	**−20.2%*****
MRI								
***Caudate volume** % TIV*	0.48 ± 0.04	−2.6%	0.37 ± 0.02	−4.2%	0.33 ± 0.05	**−7.8%****	0.29 ± 0.05	−6.2%
***Putamen volume** % TIV*	0.65 ± 0.1	3.1%	0.44 ± 0.05	**−7.0%***	0.44 ± 0.08	**−6.2%***	0.44 ± 0.06	−5.1%
Cholesterol and metabolites								
***Total cholesterol** mg/ml*	1.9 ± 0.4	**+25.8%*****	1.6 ± 0.33	**+10.9%***	1.7 ± 0.41	12.2%	1.8 ± 0.4	**+14.4%** ***
***7-Dehydrocholesterol** ng/ml*	228 ± 328	+16.1%	265 ± 267	+38.0%	387 ± 414	−0.6%	1080 ± 1233	**+48.4%*****
***Desmosterol** ng/ml*	296 ± 185	+0.7%	255 ± 99	−10.8%	389 ± 318	+34.4%	360 ± 312	+19.6%
***27-Hydroxycholesterol** ng/ml*	73.9 ± 48.0	+18.2%	68.6 ± 66.7	−11.3%	77.5 ± 48.5	+1.2%	105.7 ± 69.7	+6.0%
***24-Hydroxycholesterol** ng/ml*	36.7 ± 17.9	+4.1%	24.9 ± 9.4	−4.4%	36.8 ± 23.8	−6.2%	30.2 ± 16.2	+3.4%
Neurofilament Light Chain								
***NfL** pg/ml*	8.89 ± 4.4	+11.1%	20.27 ± 7.1	**+20.2%*****	21.25 ± 8.1	+4.7%	28.04 ± 7.4	+4.7%

Difference between Follow-up (FU) and Baseline (BL) value are indicates in percentage. Huntington disease; UHDRS: Unified Huntington Disease Rating Scale; TMS: Total motor score; TFC: Total Functional Capacities; SDMT: Symbol Digit Modalities Test; TIV: Total Intracranial Volume. *P* values: * < 0.05; ** ≤0.01; *** ≤0.005 (paired *t*-test for repeated measures).

et al., 2024).

Our study identified, through ROC analyses, an NfL threshold of 7.5 pg/mL that discriminated both HD-ISS stage 0 and HD-ISS stage 1 individuals from healthy controls. In the study by Parkin et al. (2022) the authors defined a cut-off value of 45 pg/ml for NfL to distinguish premanifest HD individuals who are within 10 years of the expected disease onset from healthy controls (Parkin et al., 2022). Although the absolute cutoff values differ from those identified in our study; our data confirm that increased NfL concentration may represent one of the early changes in plasma detectable in premanifest individuals (Byrne et al., 2017).

Interestingly, in HD-ISS-0, NfL concentrations correlated with caudate and putamen volume and with estimated years to disease onset. In our previous studies (Leoni et al., 2008; Leoni et al., 2011; Leoni et al., 2013), plasma 24S-OHC levels correlated with clinical and cognitive measures, including behavioral performance and MRI-derived striatal volumes. In the present study, such associations were not detected, likely reflecting several methodological and biological factors. In this work, we used high-sensitivity UHPLC–MS quantification, which yields highly variable raw data with large standard deviations. In addition, our sample population included a larger, and more diverse cohort compared with previous study populations, thereby reducing the likelihood of detecting marginal associations. Moreover, MRI volumetric analyses of the basal ganglia are currently obtained from more precise 3 T MRI, in which the volumes of caudate and putamen nuclei were separately evaluated. In previous studies, neuroimaging acquisitions were obtained on 1.5 T MRI (Leoni et al., 2008; Leoni et al., 2013) and correlations were performed with total striatal volume (Leoni et al., 2011). Beyond these methodological aspects; we need to consider that underlying biology of 24S-OHC; and the role of the brain-specific enzyme; CYP46A1; whose activity is crucial for brain cholesterol homeostasis. Reduction of both 24S-OHC levels and CYP46A1 protein were demonstrated in the putamen of post-mortem HD patients and in animal models of the disease (Russell et al., 2009; Valenza et al., 2023). Interestingly, in a mouse model of the disease (R6/2), the delivery of CYP46A1 in the striatum, using the AAVrh10 vector, was shown to mitigate neuronal atrophy, motor abnormalities, and huntingtin protein aggregation, suggesting a potential relationship between CYP46A1 activity and cholesterol homeostasis in HD pathogenesis (Valenza et al., 2023). Based on these data, an ongoing early phase clinical trial is currently testing the potential therapeutic effect of an AAV-based gene therapy in which CYP46A1 is delivered into the brain of HD patients (NCT05541627).In this type of study, measurement of plasma 24S-OHC levels may represent a pharmacodynamic biomarker for monitoring the effect of the experimental intervention.

In our study, we showed that reduced plasma 24S-OHC concentration may reflect neuronal loss and/or neuronal metabolic disfunction in the early clinical stage, while in more advanced stages of disease progression, the levels remain stable. NfL, in contrast, shows stronger correlations with functional and MRI measures of disease progression in both early and advanced stages. The main advantage of NfL lies in the relative simplicity and high sensitivity of the assay methods. Conversely, quantitative determination of 24S-OHC is rather complicated, and the variability of the quantitative data is considerably elevated. Consistent with our results, Asgari et al (Asgari et al., n.d.). suggested that 24S-OHC could potentially be used as a marker of pharmacodynamic response at the group level rather than as a prognostic indicator at the individual level. In this contest; molecular imaging using positron emission tomography has recently emerged as a sensitive; non-invasive alternative to assess brain cholesterol homeostasis (Haider et al., 2022).

In conclusion, NfL and 24S-OHC delineate complementary aspects of HD pathophysiology. NfL emerges as a sensitive marker of early neuroaxonal damage, capable of capturing the dynamic progression from the pre-symptomatic to the late manifest HD stages, and to monitor the safety in therapeutical interventions. The 24S-OHC reflects early and stable disturbances in brain cholesterol metabolism, and may be a useful biomarker not only for therapies targeting cholesterol metabolic pathways, but also in other therapeutic strategies, including mutant huntingting-lowering approaches.

The integration and the longitudinal evaluation of both biomarkers

may provide a powerful strategy to identify the optimal therapeutic window for intervention and to monitor treatment response in future HD clinical trials.

CRediT authorship contribution statement

Lidia Sarro: Data curation, Writing – review & editing, Writing – original draft. **Marta Valenza:** Formal analysis, Writing – review & editing, Writing – original draft. **Alessia Mongelli:** Investigation, Data curation, Writing – review & editing. **Alice Passoni:** Investigation, Data curation, Conceptualization. **Anna Castaldo:** Visualization, Investigation, Data curation. **Monica Favagrossa:** Investigation, Formal analysis, Data curation. **Laura Pasetto:** Investigation, Formal analysis, Data curation. **Valentina Bonetto:** Investigation, Formal analysis, Data curation. **Renzo Bagnati:** Investigation, Formal analysis, Data curation. **Marina Grisoli:** Supervision, Investigation. **Anna Nigri:** Investigation, Formal analysis, Data curation. **Giulia Birolini:** Formal analysis, Writing – review & editing. **Elena Zerbini:** Investigation, Data curation. **Simone Tomè:** Formal analysis, Writing – review & editing. **Marco Masseroli:** Formal analysis, Writing – review & editing. **Erika Salvi:** Formal analysis, Writing – review & editing. **Laura Colombo:** Supervision, Investigation, Formal analysis. **Mario Salmona:** Supervision, Funding acquisition, Conceptualization. **Elena Cattaneo:** Supervision, Funding acquisition, Conceptualization, Writing – review & editing. **Caterina Mariotti:** Supervision, Formal analysis, Data curation, Conceptualization, Writing – review & editing, Writing – original draft.

Funding

Grant RF-2016-02361928 to MS and RRC (Italian Ministry of Health).

Declaration of competing interest

None.

Acknowledgements

This work was supported by the Italian Ministry of Health (Grant RF-2016-02361928 to MS; and Ricerca Corrente). L.S., and C.M., are members of the European Reference Network for Rare Neurological Disorders (ERN-RND), Project ID No. 739510. We thank Mario Fichera, and Gloria Marchini for their collaboration. The paper is dedicated to the memory of our colleague Dr. Lorenzo Nanetti.

Appendix A. Supplementary data

Supplementary data to this article can be found online at https://doi.org/10.1016/j.nbd.2026.107381.

Data availability

Anonymized data that support the findings of this study and not published within this article will be made available from open repository of the Fondazione IRCCS Istituto Neurologico Carlo Besta (https://zenodo.org/communities/besta) upon reasonable request to the corresponding author.

References

A Virata, M.C., Catahay, J.A., Lippi, G., Henry, B.M., 2024. Neurofilament light chain: a biomarker at the crossroads of clarity and confusion for gene-directed therapies. Neurodegener. Dis. Manag. 14 (6), 227–239. https://doi.org/10.1080/17582024.2024.2421738.

Asgari, M.A., Langbehn, D.R., Skibinski, D.O.F., Lee, R., Griffiths, W.J., Wang, Y., 2026. 24S-hydroxycholesterol: a potential brain-derived biomarker of Huntington's Disease. medRxiv. https://doi.org/10.1101/2025.10.08.25337337 preprint.

Björkhem, I., Lütjohann, D., Diczfalusy, U., Ståhle, L., Ahlborg, G., Wahren, J., 1998. Cholesterol homeostasis in human brain: turnover of 24S-hydroxycholesterol and evidence for a cerebral origin of most of this oxysterol in the circulation. J. Lipid Res. 39 (8), 1594–1600.

Byrne, L.M., Rodrigues, F.B., Blennow, K., et al., 2017. Neurofilament light protein in blood as a potential biomarker of neurodegeneration in huntingtons disease: a retrospective cohort analysis. Lancet Neurol. 16 (8), 601–609. https://doi.org/10.1016/S1474-4422(17)30124-2.

Byrne, L.M., Rodrigues, F.B., Johnson, E.B., et al., 2018. Evaluation of mutant huntingtin and neurofilament proteins as potential markers in Huntington disease. Sci. Transl. Med. 10 (458), eaat7108. https://doi.org/10.1126/scitranslmed.aat7108.

Dorsey, E.R., 2013. Natural history of Huntington disease. JAMA Neurol. https://doi.org/10.1001/jamaneurol.2013.4408. Published online October 14.

Fischl, B., Sereno, M.I., Dale, A.M., 1999. Cortical surface-based analysis. NeuroImage 9 (2), 195–207. https://doi.org/10.1006/nimg.1998.0396.

Gamba, P., Giannelli, S., Staurenghi, E., et al., 2021. The controversial role of 24-S-hydroxycholesterol in alzheimers disease. Antioxidants 10 (5), 740. https://doi.org/10.3390/antiox10050740.

Gray, S.M., Dai, J., Smith, A.C., et al., 2024. Changes in 24(S)-hydroxycholesterol are associated with cognitive performance in early huntingtons disease: data from the TRACK and ENROLL HD cohorts. J. Huntington's Dis. 13 (4), 449–465. https://doi.org/10.3233/JHD-240030.

Haider, A., Zhao, C., Wang, L., et al., 2022. Assessment of cholesterol homeostasis in the living human brain. Sci. Transl. Med. 14 (665), eadc9967. https://doi.org/10.1126/scitranslmed.adc9967.

Huang, X., Sterling, N.W., Du, G., et al., 2019. Brain cholesterol metabolism and parkinsons disease. Mov. Disord. 34 (3), 386–395. https://doi.org/10.1002/mds.27609.

Johnson, E.B., Byrne, L.M., Gregory, S., et al., 2018. Neurofilament light protein in blood predicts regional atrophy in Huntington disease. Neurology 90 (8). https://doi.org/10.1212/WNL.0000000000005005.

Khalil, M., Teunissen, C.E., Otto, M., et al., 2018. Neurofilaments as biomarkers in neurological disorders. Nat. Rev. Neurol. 14 (10), 577–589. https://doi.org/10.1038/s41582-018-0058-z.

Langbehn, D., Brinkman, R., Falush, D., Paulsen, J., Hayden, M., On behalf of an international huntingtons disease collaborative group, 2004. A new model for prediction of the age of onset and penetrance for huntingtons disease based on CAG length. Clin. Genet. 65 (4), 267–277. https://doi.org/10.1111/j.1399-0004.2004.00241.x.

Langbehn, D.R., Hayden, M.R., Paulsen, J.S., the PREDICT-HD Investigators of the Huntington Study Group, 2010. CAG-repeat length and the age of onset in Huntington disease (HD): a review and validation study of statistical approaches. Am. J. Med. Genet. B Neuropsychiatr. Genet. 153B (2), 397–408. https://doi.org/10.1002/ajmg.b.30992.

Lee, J.M., Correia, K., Loupe, J., et al., 2019. CAG repeat not polyglutamine length determines timing of huntingtons disease onset. Cell 178 (4). https://doi.org/10.1016/j.cell.2019.06.036, 887–900.e14.

Leoni, V., Mariotti, C., Tabrizi, S.J., et al., 2008. Plasma 24S-hydroxycholesterol and caudate MRI in pre-manifest and early huntingtons disease. Brain 131 (11), 2851–2859. https://doi.org/10.1093/brain/awn212.

Leoni, V., Mariotti, C., Nanetti, L., et al., 2011. Whole body cholesterol metabolism is impaired in huntingtons disease. Neurosci. Lett. 494 (3), 245–249. https://doi.org/10.1016/j.neulet.2011.03.025.

Leoni, V., Long, J.D., Mills, J.A., Di Donato, S., Paulsen, J.S., 2013. Plasma 24S-hydroxycholesterol correlation with markers of Huntington disease progression. Neurobiol. Dis. 55, 37–43. https://doi.org/10.1016/j.nbd.2013.03.013.

Li, X.-Y., Bao, Y.-F., Xie, J.-J., Gao, B., Qian, S.-X., Dong, Y., Wu, Z.-Y., 2023. Application value of serum neurofilament light protein for disease staging in huntingtons disease. Mov. Disord. 38 (7), 1307–1315, 10.1002/mds.29430.

Locci, S., Nidiaci, V., De Stefano, N., Leoni, V., Mignarri, A., 2022. 24S-hydroxycholesterol and cerebellar degeneration: Insights from SCA2. Cerebellum 22 (5), 1020–1022. https://doi.org/10.1007/s12311-022-01448-7.

Marder, K., Zhao, H., Myers, R.H., et al., 2000. Rate of functional decline in huntingtons disease. Neurology 54 (2). https://doi.org/10.1212/WNL.54.2.452, 452–452.

Miller, T.M., Cudkowicz, M.E., Genge, A., et al., 2022. Trial of antisense oligonucleotide tofersen for SOD1 ALS. N. Engl. J. Med. 387 (12), 1099–1110. https://doi.org/10.1056/NEJMoa2204705.

Parkin, G.M., Corey-Bloom, J., Snell, C., Castleton, J., Thomas, E.A., 2021. Plasma neurofilament light in huntingtons disease: a marker for disease onset, but not symptom progression. Parkinsonism Relat. Disord. 87, 32–38. https://doi.org/10.1016/j.parkreldis.2021.04.017.

Parkin, G.M., Corey-Bloom, J., Long, J.D., Snell, C., Smith, H., Thomas, E.A., 2022. Associations between prognostic index scores and plasma neurofilament light in huntingtons disease. Parkinsonism Relat. Disord. 97, 25–28. https://doi.org/10.1016/j.parkreldis.2022.02.023.

Parkin, G.M., Thomas, E.A., Corey-Bloom, J., 2023. Plasma NfL as a prognostic biomarker for enriching HD-ISS stage 1 categorisation: a cross-sectional study. eBioMedicine 93, 104646. https://doi.org/10.1016/j.ebiom.2023.104646.

Parkin, G.M., Thomas, E.A., Corey-Bloom, J., 2024. Mapping neurodegeneration across the huntingtons disease spectrum: a five-year longitudinal analysis of plasma neurofilament light. eBioMedicine 104, 105173. https://doi.org/10.1016/j.ebiom.2024.105173.

Passoni, A., Favagrossa, M., Valenza, M., et al., 2024. A cutting-edge approach based on UHPLC-MS to simultaneously investigate oxysterols and cholesterol precursors in biological samples: validation in huntingtons disease mouse model. Talanta Open. 9, 100278. https://doi.org/10.1016/j.talo.2023.100278.

Rodrigues, F.B., Byrne, L.M., Tortelli, R., et al., 2020. Mutant huntingtin and neurofilament light have distinct longitudinal dynamics in Huntington disease. Sci. Transl. Med. 12 (574), eabc2888. https://doi.org/10.1126/scitranslmed.abc2888.

Rodrigues, F.B., Byrne, L.M., Lowe, A.J., et al., 2021. Kynurenine pathway metabolites in cerebrospinal fluid and blood as potential biomarkers in huntingtons disease. J. Neurochem. 158 (2), 539–553. https://doi.org/10.1111/jnc.15360.

Rosengren, L.E., Karlsson, J., Karlsson, J., Persson, L.I., Wikkelsø, C., 1996. Patients with amyotrophic lateral sclerosis and other neurodegenerative diseases have increased levels of neurofilament protein in CSF. J. Neurochem. 67 (5), 2013–2018. https://doi.org/10.1046/j.1471-4159.1996.67052013.x.

Russell, D.W., Halford, R.W., Ramirez, D.M.O., Shah, R., Kotti, T., 2009. Cholesterol 24-hydroxylase: an enzyme of cholesterol turnover in the brain. Annu. Rev. Biochem. 78 (1), 1017–1040. https://doi.org/10.1146/annurev.biochem.78.072407.103859.

Scahill, R.I., Zeun, P., Osborne-Crowley, K., et al., 2020. Biological and clinical characteristics of gene carriers far from predicted onset in the huntingtons disease young adult study (HD-YAS): a cross-sectional analysis. Lancet Neurol. 19 (6), 502–512. https://doi.org/10.1016/S1474-4422(20)30143-5.

Scahill, R.I., Farag, M., Murphy, M.J., et al., 2025. Somatic CAG repeat expansion in blood associates with biomarkers of neurodegeneration in huntingtons disease decades before clinical motor diagnosis. Nat. Med. 31 (3), 807–818. https://doi.org/10.1038/s41591-024-03424-6.

Shoulson, I., Fahn, S., 1979. Huntington disease: clinical care and evaluation. Neurology 29 (1). https://doi.org/10.1212/WNL.29.1.1, 1–1.

Tabrizi, S.J., Schobel, S., Gantman, E.C., et al., 2022. A biological classification of huntingtons disease: the integrated staging system. Lancet Neurol. 21 (7), 632–644. https://doi.org/10.1016/S1474-4422(22)00120-X.

Tripodi, D., Vitarelli, F., Spiti, S., Leoni, V., 2024. The diagnostic use of the plasma quantification of 24S-hydroxycholesterol and other oxysterols in neurodegenerative disease. In: Lizard, G. (Ed.), Implication of Oxysterols and Phytosterols in Aging and Human Diseases, Vol 1440. Springer International Publishing, pp. 337–351. https://doi.org/10.1007/978-3-031-43883-7_17. Advances in Experimental Medicine and Biology.

Valenza, M., Birolini, G., Cattaneo, E., 2023. The translational potential of cholesterol-based therapies for neurological disease. Nat. Rev. Neurol. 19 (10), 583–598. https://doi.org/10.1038/s41582-023-00864-5.

Voysey, Z.J., Owen, N.E., Holbrook, J.A., et al., 2024. A 14-year longitudinal study of neurofilament light chain dynamics in premanifest and transitional huntingtons disease. J. Neurol. 271 (12), 7572–7582. https://doi.org/10.1007/s00415-024-12700-x.

Warner, J.H., Long, J.D., Mills, J.A., et al., 2022. Standardizing the CAP score in huntingtons disease by predicting age-at-onset. J. Huntington's Dis. 11 (2), 153–171. https://doi.org/10.3233/JHD-210475.